Tellus (2002), 54A, 44–55
Printed in UK. All rights reserved

TELLUS
ISSN 0280–6495

A teleconnection pattern in upper-level meridional wind over the North African and Eurasian continent in summer

By RI-YU LU[1]*, JAI-HO OH[2] and BAEK-JO KIM[2], [1]*Institute of Atmospheric Physics, Chinese Academy of Sciences, Beijing, China;* [2]*Meteorological Research Institute, Korea Meteorological Administration, Seoul, Korea*

(Manuscript received 8 September 2000; in final form 27 August 2001)

ABSTRACT

One-point correlation analysis on upper-level meridional wind identified the existence of a teleconnection pattern in July, which emerges from North Africa to East Asia along the westerly jet in the middle latitudes. We examined the spatial and temporal structures of this teleconnection pattern, and found the unique characteristics rather different from the patterns in other elements such as geopotential height, streamfunction and vorticity. We also investigated the relationship between this teleconnection and precipitation, and suggested that the teleconnection is a possible linkage of the EASM to the Indian monsoon, and even to subtropical heating anomalies over Atlantic.

1. Introduction

Along the upper-level westerly jets, there are teleconnection patterns and stationary Rossby waves in boreal winter (Hoskins and Ambrizzi, 1993; Hsu and Lin, 1992). By an observational study, Hsu and Lin (1992) found a wave-like structure in winter that propagates downstream along the southern Eurasian continent and along an arc in the North Pacific. Hoskins and Ambrizzi (1993) confirmed such a Rossby wave propagation by the response of a barotropic model to localized forcing.

However, studies on teleconnections in boreal summer are relatively fewer. Ambrizzi et al. (1995) extended the theoretical and observational studies of winter teleconnections by Hoskins and Ambrizzi (1993) and Hsu and Lin (1992) to summer, and found a weak waveguide belt along the westerly jet stream around the whole Northern Hemisphere. In addition, some studies showed that there is a wave pattern of the correlation coefficients between the Indian summer monsoon (hereafter signified as ISM) rainfall (from June to September) and 200-hPa meridional wind in May, i.e., the interannual variability of ISM is associated with a wave pattern of meridional wind just prior to onset of ISM (e.g., Parthasarathy et al., 1991; Joseph and Srinivasan, 1999). Joseph and Srinivasan (1999) suggested that a Rossby wave is induced by the anomalous heat sources in the Bay of Bengal and adjoining regions in May.

In the previous studies on teleconnections and Rossby waves, a few variables have been used, such as geopotential heights at 500 hPa (e.g., Wallace and Gutzler, 1981), streamfunction at 200 hPa (Hsu and Lin, 1992) and vorticity (Hoskins and Ambrizzi, 1993). Anomalies of these elements are zonally elongated at the upper troposphere, because of great seasonal and interannual variabilities in meridional position of the westerly jet stream. Thus, the meridional shifts of jet stream

* Corresponding author.
Address: Institute of Atmospheric Physics, Chinese Academy of Sciences, PO Box 2718, Beijing 100080, China.
e-mail: lr@lasg.iap.ac.cn

may make the zonally oriented teleconnections or Rossby waves undistinguishable. Compared to above-mentioned elements, the meridional velocity is much less influenced by the meridional shifts of the jet stream, and may depict better the zonally oriented teleconnections. Therefore, in the present study, the meridional velocity field is used to analyze teleconnections.

The stationary waves along jet streams may be a possible mechanism responsible for the relationship between the East Asian summer monsoon (hereafter signified as EASM) and ISM rainfall, which has not been clarified yet (Guo and Wang, 1988; Kripalani and Singh, 1993). It has been believed that the disturbances in the middle latitudes may influence both the EASM (Tao and Chen, 1987) and ISM (Joseph and Srinivasan, 1999). Unfortunately, such a possible influence has not been well clarified due to the chaotic characteristics of midlatitude disturbances. Therefore, the main purpose of the present study is to examine the existence and structure of midlatitude teleconnection in meridional wind in the Northern Hemisphere summer, and to investigate the possible links between the teleconnections and monsoons.

2. Data and basic climatological features of 200-hPa horizontal winds

In this study we used the daily and monthly data from the National Centers for Environmental Prediction/National Center for Atmospheric Research (NCEP/NCAR) reanalysis (Kalnay et al., 1996). Data are on the 2.5° longitude × 2.5° latitude grid. This dataset is for 41 years from 1958 to 1998. The daily data were specially used in lag-correlation in this study.

The reanalysis precipitation is based on the model physics rather than based on rain gauge, radar or satellite estimates of precipitation. In general, model parameterizations of clouds and precipitation are generally considered to be two of the most uncertain areas in atmospheric modeling. Therefore, we utilized the independent estimates of precipitation data based on gauge observations and satellite estimates (Xie and Arkin, 1997). The length of this dataset is 20 years from 1979 to 1998. The precipitation field in NCEP/NCAR reanalysis data was also used because of the short available period of the gauge-satellite merged rainfall data.

Figure 1 shows the 200-hPa climatological zonal and meridional velocities in July. 200 hPa is approximately a level of strongest westerly jets. At this level, a jet stream with maximum zonal velocity of 20–30 m/s emerges from North Africa and extends eastwards to the North Pacific. Its axis is located over the North African and Eurasian continent in nearly zonal direction, and curves northeastward into the central Pacific. Northerlies and southerlies appear alternatively in the middle latitudes, while northerlies dominate in the tropics.

Most analyses in this study are performed at 200 hPa. The results at other upper levels exhibit a good similarity, which is partly shown and discussed in the following section (Figs. 4 and 5).

3. Teleconnection patterns along the North African–Asian westerly jet

In this section, correlation analysis is applied to investigate the existence of teleconnection in meridional wind in the Northern Hemisphere in July. Figure 2 shows the correlation between 200-hPa meridional velocity at base point (105°E, 42.5°N) and that at every point in the Northern Hemipshere. A clear wave-like structure appears over the Eurasian continent from Northwest Africa to East Asia. The central points from west to east are (10°W, 22.5°N), (15°E, 25°N), (50°E, 37.5°N), (77.5°E, 35°N), (105°E, 42.5°N) and (132.5°E, 37.5°N), respectively. The wave train is along the upper-level jet stream over the North African and Eurasian continent (Fig. 1a), and does not show an association with the climatological meridional velocity (Fig. 1b). Interestingly, this spatial distribution is considerably similar to the correlation between the ISM rainfall and 200-hPa meridional wind in May (Fig. 5 of Joseph and Srinivasan, 1999) in Eurasian continent.

Compared to the Rossby wave during winter (Hoskins and Ambrizzi, 1993; Hsu and Lin, 1992), the present result shows a slightly larger zonal wavenumber and poleward displacement, possibly due to the weakness and poleward shift of the upper-level westerly jet stream in summer. These differences between winter and summer are in

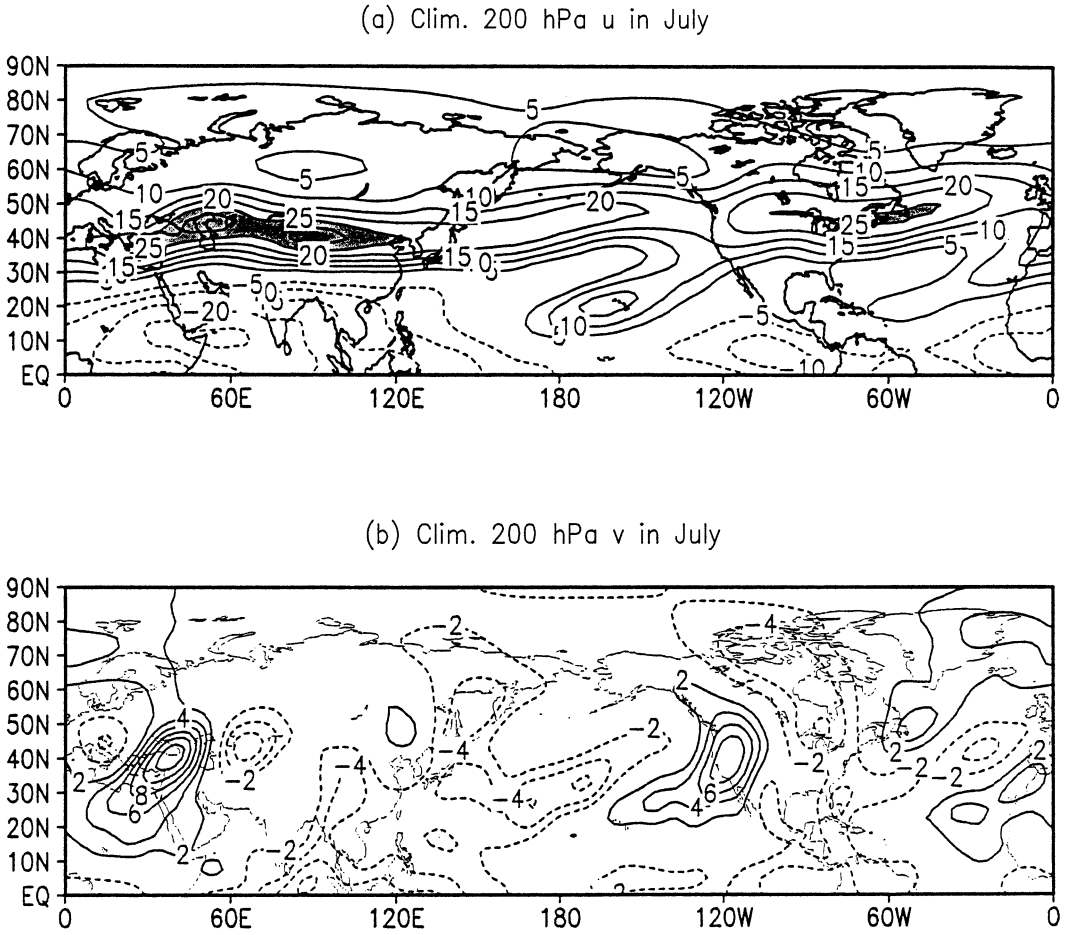

Fig. 1. Climatological zonal (a) and meridional (b) velocities at 200 hPa in July, averaged over 1958–1998. Units m/s. Contour interval is 5 and 2 in (a) and (b), respectively. Zero contour is not shown. Positive values larger than 25 are shaded in (a).

good agreement with the June–July–August (JJA) results of Ambrizzi et al. (1995), who showed that the zonal wavenumber over the Eurasian continent is about 7 for JJA, larger than 5 for December–January–February (DJF), and that the strong North African–Asian waveguide in JJA moves some 10° poleward, compared to DJF.

Actually, one of centers of our wave pattern is almost exactly the base point (75°E, 35°N) used by Ambrizzi et al. (1995) in their Fig. 7, but their wave pattern disappears west of the Arabian Peninsula. In addition, the teleconnection pattern in meridional wind shows a clearer structure than that in Ambrizzi et al. (1995) (see their Fig. 7).

The meridional velocity in this wave structure is well related with zonal velocity. Figure 3 shows the correlation between 200-hPa meridional velocity at the base point and zonal velocity at every point. Three major regions with significantly negative correlation are East Asia, Iran and the Northwest Africa, respectively. Due north of these regions, there are three corresponding regions of positive correlation. The north–south dipole-like locations of correlation indicate that the meridional velocity around (105°E, 42.5°N) is related well with the meridional displacement of the upper-level jet stream over East Asia, Iran and the Northwest Africa. Figures 2 and 3 together

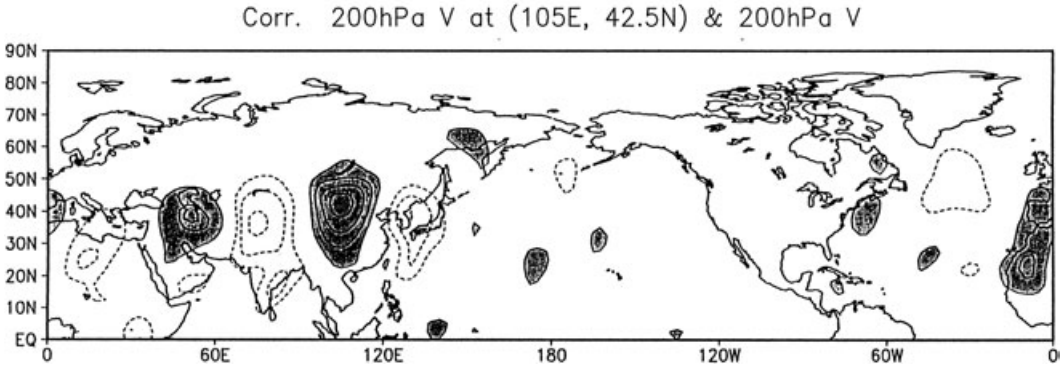

Fig. 2. Correlation coefficients between meridional velocity at base point (105°E, 42.5°N) and that at every point at 200 hPa. Contour lines of ± 0.3, ± 0.5, ± 0.7 and ± 0.9 are shown. The shading illustrates the significance at the 95% level (absolute values of correlation coefficients larger than 0.3 with sample number of 41). Positive and negative values are heavily and lightly shaded, respectively.

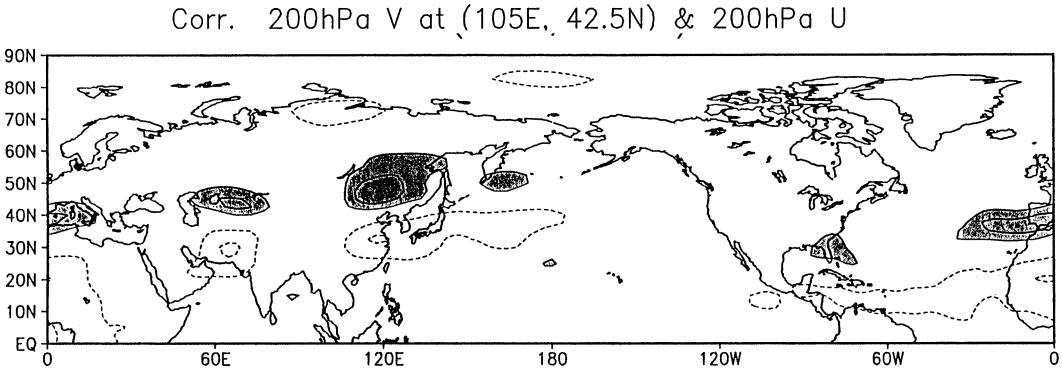

Fig. 3. Same as Fig. 2, but for zonal velocity at every point.

suggest that associated with a southerly anomaly at the point (105°E, 42.5°N), there are three anticyclonic anomalies over East Asia, Iran and Northwest Africa, respectively. These anticyclonic anomalies are coincidentally located at the northwest sides of monsoons, i.e., East Asian, Indian and African monsoons, respectively.

Figure 4 shows the correlation coefficients between meridional velocity at the base point (105°E, 42.5°N) and that at every point at 400 hPa and at 500 hPa, respectively. The teleconnection pattern at 400 hPa is strikingly similar to that at 200 hPa (Fig. 2), but at the slightly lower level (500 hPa) it becomes remarkably unclear over the North African and Eurasian continent while seems to be a little more clearer over the North Pacific. The considerable differences of the teleconnection patterns are suggested to be due to the significant difference in zonal velocity between the two levels (Fig. 5). At 400 hPa, a westerly jet stream goes through over the Eurasian continent, similar to but slightly weaker than that at 200 hPa (Fig. 1a). At 500 hPa, however, the westerly jet stream becomes remarkably weaker, with its maximum velocity being approximately half of that at 400 hPa. At and below 500 hPa, the westerly tends to appear over the oceans rather than the continents, in contrast to that at upper levels. We suggest that the strong upper-level westerly jet provides a waveguide, and that the remarkable weakness in the 500-hPa westerly jet over the Eurasian continent does not provide favourable background flows for the existence of any teleconnection patterns that are clearly trapped along the jet.

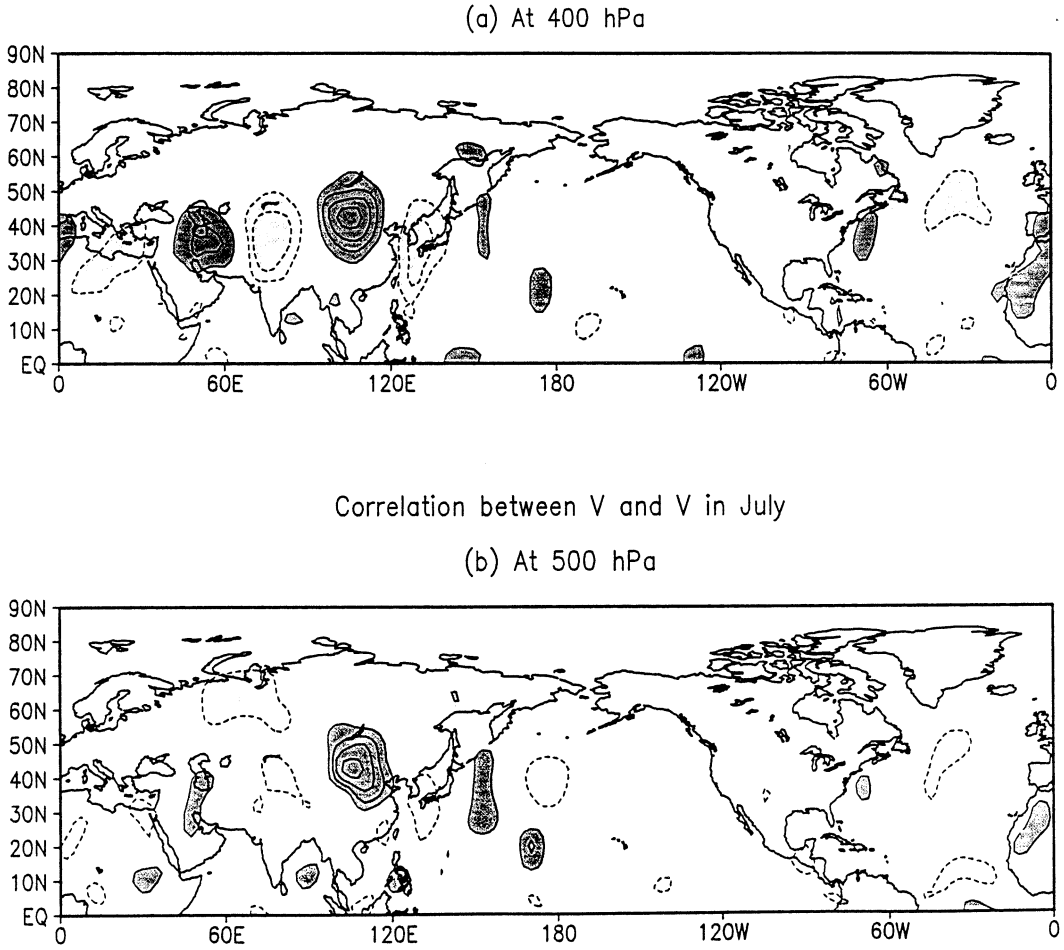

Fig. 4. Correlation coefficients between meridional velocity at the base point (105°E, 42.5°N) and that at every point at 400 hPa (a) and at 500 hPa (b). Contour lines of ± 0.3, ± 0.5, ± 0.7 and ± 0.9 are shown. The shading illustrates the significance at 95% level. Positive and negative values are heavily and lightly shaded, respectively.

4. Unique characteristics of the teleconnection pattern deduced in meridional wind field

The previous studies demonstrated that the characteristics of teleconnection patterns are strongly dependent on the timescales (Blackmon et al., 1984a, b; Hsu and Lin, 1992; Kiladis and Weickmann, 1992). In summary, the fluctuations with long timescales (periods longer than 30 days) exhibit geographically fixed north–south dipole patterns straddling the jet exit regions. The signals with the intermediate timescales (periods of 10–30 days) are dominated by mobile wave trains oriented along waveguides in the westerly jet streams. The time variation of the fluctuations with the intermediate timescales shows the successive downstream development of new centers of action, with each center remaining almost stationary. This phenomenon is interpreted by the two-dimensional Rossby-wave dispersion.

The teleconnection pattern in meriodional wind in the present study should exhibit the features of low-frequency band (periods longer than 30 days), since the monthly mean data were used. Actually, the teleconnection pattern in meridional wind is geographically fixed. If the base point is moved to the longitude of 120°E, there is not a clear wave-

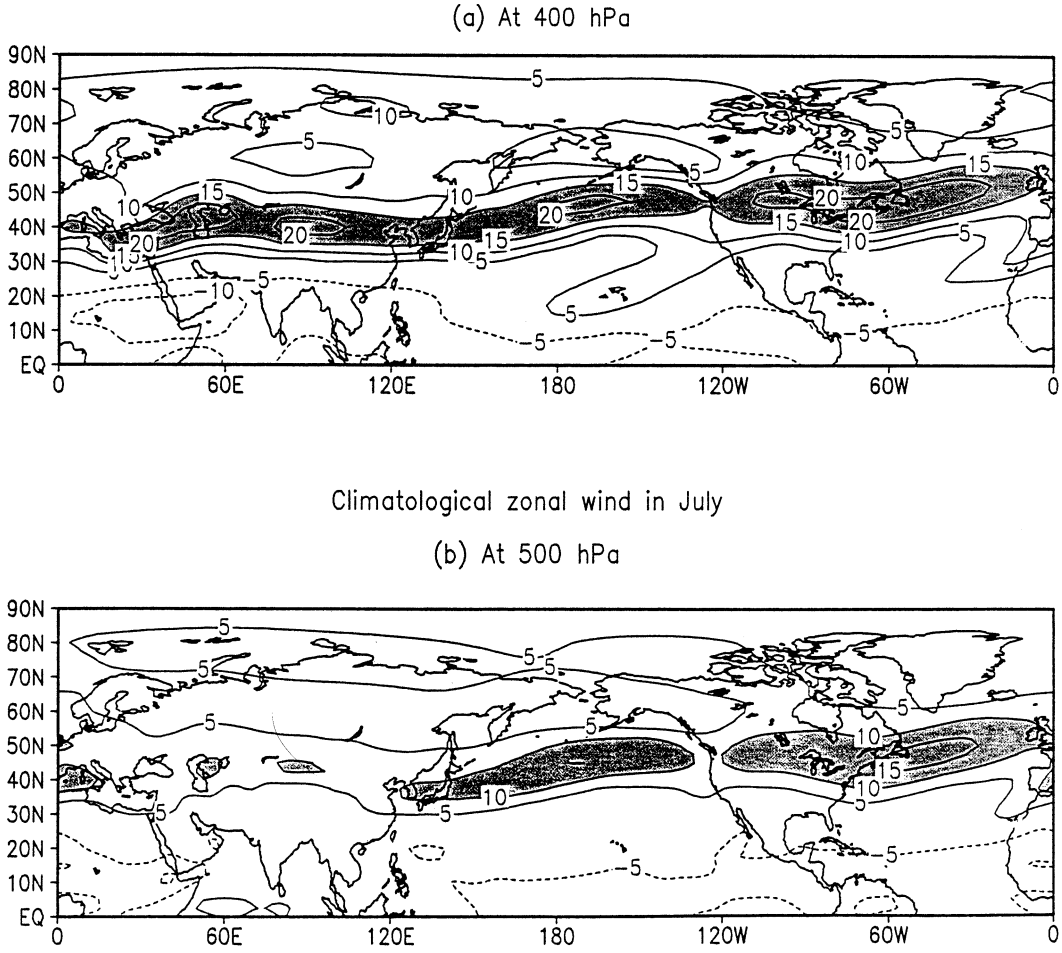

Fig. 5. Climatological zonal velocities in July at 400 hPa (a) and at 500 hPa (b). Units m/s. The contour interval is 5. The zero contour is not shown. Positive values larger than 15 and 10 are shaded in (a) and (b), respectively.

like pattern no matter how the base point is shifted latitudinally (not shown). The standard deviation of meridional wind (Fig. 6) also suggests a geographically fixed teleconnection pattern. There are two bands of large standard deviations with localized maxima over the Eurasian continent, one over the northern Eurasian continent and another along the latitude of 40°N where the westerly jet stream is located in July (Fig. 1a). The points with larger standard deviation along the westerly jet are strikingly consistent with the central points of the teleconnection pattern in meridional wind with the exception of that over the Korean peninsula (Fig. 2), indicating that the meridional wind exhibits the greatest interannual variability at the central points of the teleconnection pattern. The fact that the meridional wind exhibits greatest interannual variability at the geographically fixed points favors the appearance of a geographically fixed teleconnection pattern.

On the other hand, the fact that the teleconnection pattern in meridional wind is oriented along the North African–Asian waveguide with the zonal wavenumber of about 7 indicates that this teleconnection pattern is similar to those in the intermediate-frequency band. The zonally oriented wave-like structure changes very slightly even when the JJA averages or the averages over

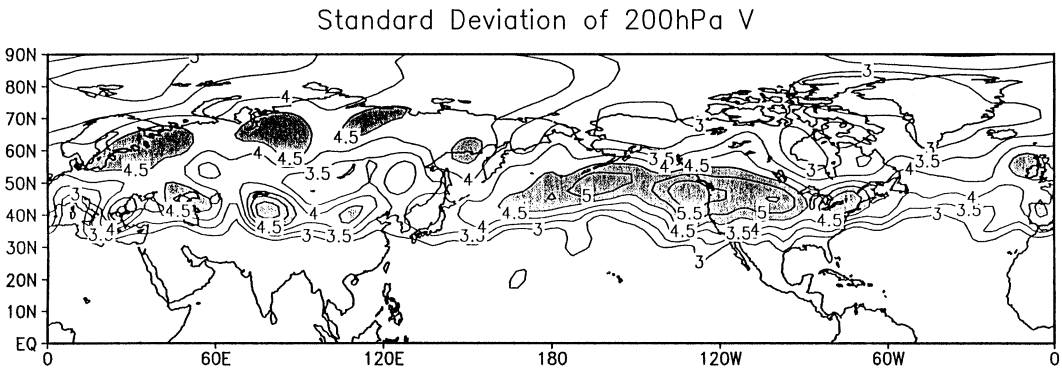

Fig. 6. Standard deviation of July mean meridional wind at 200 hPa. The contour interval is 0.5 m/s. Values less than 3 are not shown and larger than 4.5 are shaded.

a shorter period, such as 15-day mean, are used in the analysis on teleconnection (not shown). Therefore, the teleconnection pattern in meridional wind appears not to be related to period bands, unlike those in other elements, such as geopotential height, streamfunction and vorticity, that have been widely used in the previous studies (Wallace and Gutzler, 1981; Blackmon et al., 1984a, b; Kiladis and Weickmann, 1992; Hsu and Lin, 1992; Hoskins and Ambrizzi, 1993; Ambrizzi et al., 1995).

It was shown by lag-correlation statistics that the fluctuations with the intermediate timescales are characterized by the successive downstream development of new centers of action, with each center remaining almost stationary (Blackmon et al., 1984a, b; Kiladis and Weickmann, 1992; Hsu and Lin, 1992; Hoskins and Ambrizzi, 1993; Ambrizzi et al., 1995). To compare with these previous results, we carried out the lag-correlation analysis on meridional wind field. Figure 7 shows the lag-correlation patterns for the 200-hPa meridional wind for lags of -15 and $+15$ days relative to fluctuations at the base point (105°E, 42.5°N). For lag of –15 days relative to fluctuations at the base point, we calculated the correlation coefficients between the July monthly mean data at the base point and 16 June–16 July (also 31 days) mean data at every point. Likewise, for lag of 15 days, we calculated the correlation coefficients between the July monthly mean data at the base point and 16 July–15 August (also 31 days) mean data at every point. The -15 day lag-correlation pattern (Fig. 7a) is almost identical to the simultaneous correlation one (Fig. 2). In the $+15$ day lag-correlation pattern (Fig. 7b), the wave-like structure is concentrated over the central Asia and East Asia, without any significant correlation west of the Mediterranean Sea. The $+15$ day lag correlation over the Korea and Japan appears to be stronger than the simultaneous one. However, the teleconnection pattern appears to be trapped over East Asia, showing no significant lag-correlation east of East Asia. We also examined the lag-correlation patterns for ± 5, ± 10, ± 20, ± 25 and ± 30 days, respectively (not shown), and found that the patterns are somewhat similar with those for the lags of ± 15 days when the lag time is less than 15 days, but lose its clear wave-like structure when the lag time is more than 15 days.

These results by lag-correlation suggest that there are differences between the present teleconnection pattern and the ones on intermediate timescales in the previous studies, although all of them show the wave-like structure along waveguides of jet streams. Therefore, the teleconnection pattern in meridional wind exhibits its unique characteristics. On the one hand, this teleconnection pattern appears not to be related to period bands, whereas those in other elements such as geopotential heights, streamfunction and vorticity are strongly dependent on period bands (Blackmon et al., 1984a, b; Kiladis and Weickmann, 1992; Hsu and Lin, 1992). On the other hand, the teleconnection pattern in meridional wind exhibits basically mixed features of patterns in other elements on both long and intermediate timescales, and the unique mode of

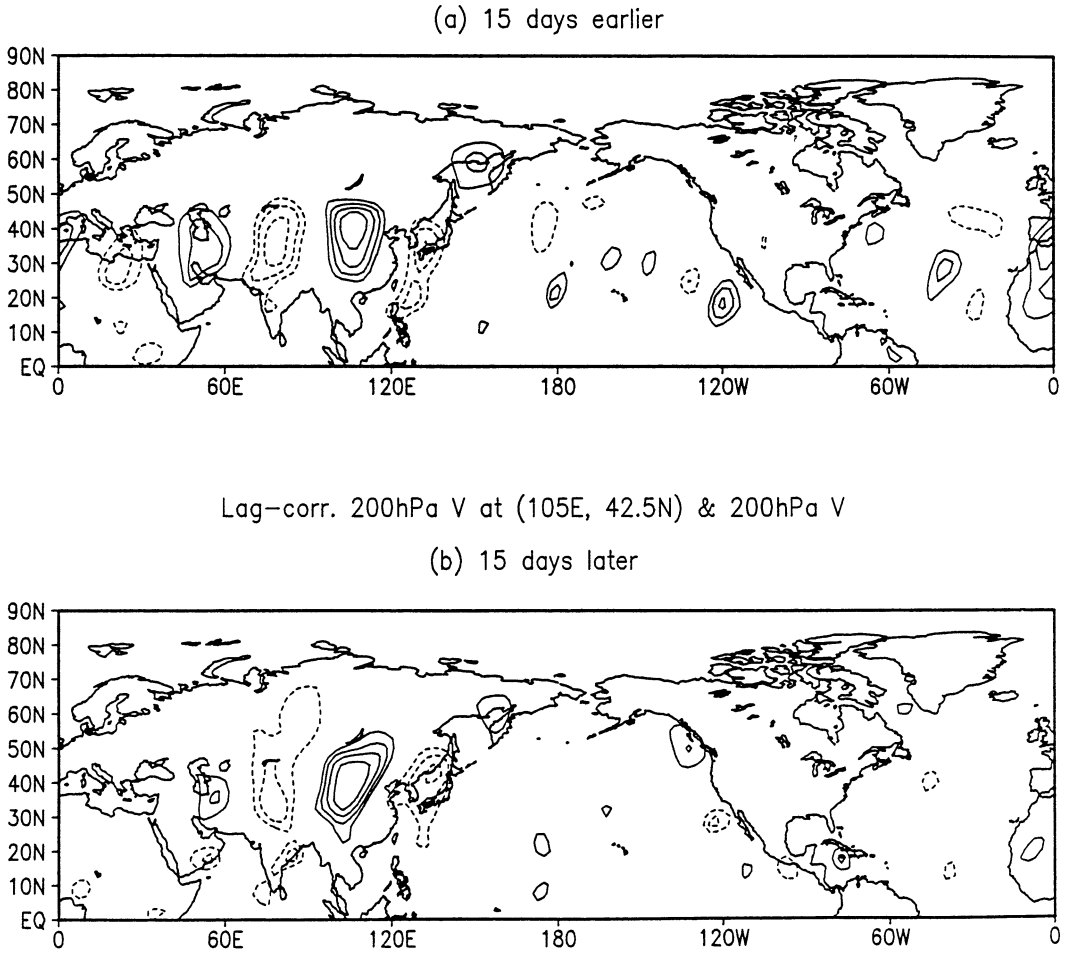

Fig. 7. Lag-correlation patterns for the 200-hPa meridional wind for lags of (a) −15 and (b) +15 days relative to fluctuations at the base point (105°E, 42.5°N). Contour lines of ±0.3, ±0.5, ±0.7 and ±0.9 are shown. The shading illustrates the significance at 95% level.

lag-correlation patterns. In addition, the teleconnection pattern in meridional wind is much clearer than those in other elements.

The following discussion is given to explain the reason for the clearer wave-like structure of the teleconnection pattern in meridional wind than those in other elements. The elements used in the previous studies, such as geopotential height, streamfunction and vorticity, are all closely related to zonal wind while related to meridional wind to a very small extent at the middle and upper troposphere in the middle latitudes, since the meridional velocity is much smaller than zonal one. The zonal wind, however, exhibits a considerable seasonal evolution and thus its low-frequency component is dominant, resulting in the teleconnection patterns straddling the midlatitude jets on the long timescales. Therefore, the elements closely related to the zonal wind tend to exhibit zonally elongated fluctuations, which mask zonally oriented signals. Therefore, these elements have a lower ability in depicting zonally oriented teleconnections.

In the studies by simple models (Hoskins and Ambrizzi, 1993; Ambrizzi et al., 1995), the seasonal mean flows are used, and thus there is no seasonal evolution. Therefore, the Rossby waves deduced in vorticity are characterized by the zonally

oriented patterns, which are similar to the teleconnection pattern identified in this study but unlike the teleconnection patterns deduced in observation at the long band.

5. Heat sources associated with the teleconnection pattern

Joseph and Srinivasan (1999) suggested that the quasi-stationary Rossby waves are induced by heat sources. In this section we examine precipitation and surface temerature, which are related to diabatic heating. Figure 8 shows the correlation coefficients between the 200-hPa meridional velocity at the base point (105°E, 42.5°N) and model-produced precipitation rate. Corresponding to a southerly at the base point at 200 hPa, there is more precipitation in central North China and less precipitation in the EASM region, i.e., the basin of the Yangtze and Huaihe Rivers in China (roughly 110–120°E, 29–34°N), Korea and central and southern Japan. In addition, there are more precipitations over India and tropical North Atlantic. Both in-phase precipitation between India and central North China and out-of-phase between India and EASM region are in agreement with the previous results by direct correlation analyses on the gauge rainfall data (Guo and Wang, 1988; Kripalani and Singh, 1993).

There is a noticeable difference between the observed and model-produced precipitations (Annamalai et al., 1999). Therefore, it is necessary to re-examine the above results by observed precipitations. We used the gauge-satellite merged rainfall data for 20 years from 1979 to 1998 to re-examine the correlation between the 200-hPa meridional velocity and precipitation (Fig. 9). Figure 9 shows a similar distribution with that obtained from model-produced rainfall data (Fig. 8), with a noticeable difference in significance level in India and the equatorial central Pacific. It supports the above-mentioned correlations obtained from model-produced rainfall.

The precipitation anomaly in the tropical North Atlantic is possibly associated with poleward displacement of the intertropical convergence zone (ITCZ), and with the sea surface temperature anomalies (SSTAs) (Fig. 10). Another significantly positive correlation appears in the EASM region and extends poleward into Northeast China, i.e., a southerly at the base point corresponds to higher surface temperatures in these regions, which is likely due to the lower precipitation there.

This study suggests that the teleconnection pattern along the westerly jet stream in the middle latitudes plays a possible role in linking the EASM and ISM, and many previous studies indicated that the ENSO affects both EASM and ISM. However, there is no systematic and significant relation between the teleconnection and SSTAs in the equatorial eastern Pacific. Therefore, the teleconnection pattern identified in this study and ENSO events in the tropics are possibly two independent factors influencing the EASM and ISM.

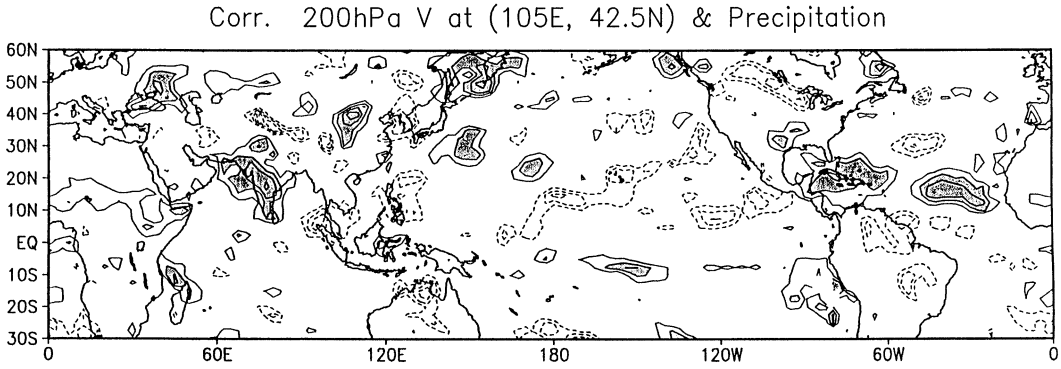

Fig. 8. Correlation coefficients between 200-hPa meridional velocity at the base point (105°E, 42.5°N) and model-produced precipitations at every point. Contour interval is 0.1, but lines of 0 and ± 0.1 are not shown. The shading illustrates the significance at 95% level, with positive and negative values being heavily and lightly shaded, respectively.

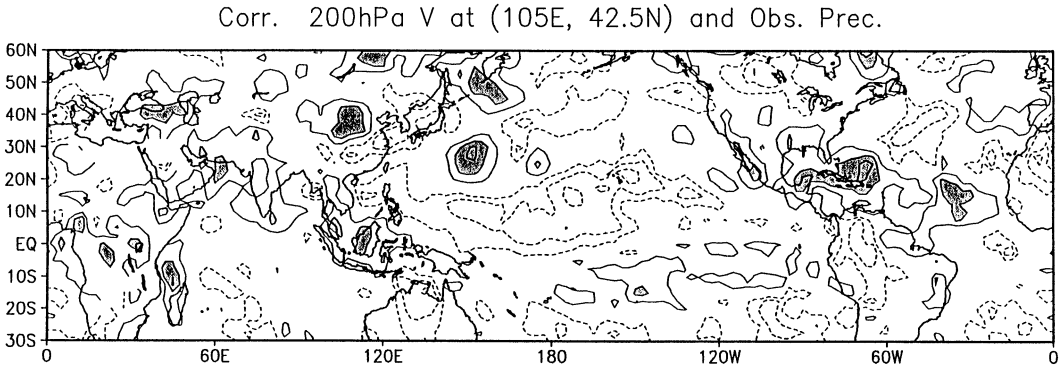

Fig. 9. Correlation coefficients between 200-hPa meridional velocity at the base point (105°E, 42.5°N) and model-produced precipitations at every point. Contour interval is 0.1, but lines of 0 and ± 0.1 are not shown. The shading illustrates the significance at 95% level, with positive and negative values being heavily and lightly shaded, respectively.

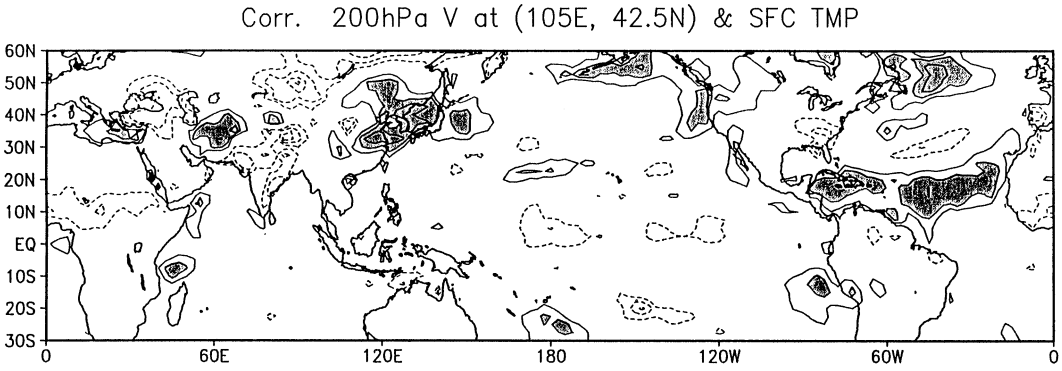

Fig. 10. Same as Fig. 8, but for surface temperature at every point.

6. Conclusions and discussion

Data used in this study include the NCEP/NCAR reanalysis data and independent gauge and satellite merged precipitation data. We found a wave train by correlation analysis on the interannual variations of July upper-level meridional velocity. The wave train is trapped along the upper-level jet stream over the North African and Eurasian continent. Compared with the Rossby waves during winter (Hoskins and Ambrizzi, 1993; Hsu and Lin, 1992), the wave train found in this study exhibits a slightly larger zonal wavenumber and poleward displacement, possibly due to the weakness and poleward shift of jet stream in summer. These differences between winter and summer are in agreement with the JJA results by Ambrizzi et al. (1995). Actually, the present results showed a similarity to one of wave patterns presented by Ambrizzi et al. (1995), but with a considerably clearer structure. This similarity suggests that the theory addressed by Hoskins and Ambrizzi (1993) and Ambrizzi et al. (1995) may apply to the present findings.

The teleconnection pattern in meridional wind is found to exhibit its unique characteristics. On the one hand, it appears not to be related to period bands, whereas those in other elements such as geopotential heights, streamfunction and vorticity are strongly dependent on period bands (Blackmon et al., 1984a, b; Kiladis and Weickmann, 1992; Hsu and Lin, 1992). On the other hand, the teleconnection pattern in meridional wind exhibits many features mixed from

patterns in other elements on both long and intermediate timescales, which is summarized in Table 1. In addition, lag-correlation shows that the teleconnection pattern seems to be trapped over East Asia, which is also one of the unique features.

The teleconnection pattern identified in this study has a much clearer structure than the patterns in the previous studies. The elements used in the previous studies are all closely related to zonal wind at the middle and upper troposphere in the middle latitudes. The zonal wind shows a great seasonal variability in its meridional location, and tends to make the fluctuation signals zonally elongated. Therefore, the elements related closely to zonal wind have a lower ability in depicting zonally oriented teleconnections.

There is no seasonal evolution in the simple model studies, since the seasonal mean flows are used (Hoskins and Ambrizzi, 1993; Ambrizzi et al., 1995). Therefore, the Rossby waves deduced in vorticity are characterized by the zonally oriented patterns, which are similar to the teleconnection pattern identified in this study but unlike those deduced in observation at the long band.

This wave train shows a significant correlation with the EASM and ISM but with different signs. It also shows a significant correlation with precipitation and SSTs in the tropical Atlantic Ocean. These correlations suggest the upper-level teleconnection's possible role in linking the EASM to ISM, and even to further westward heat sources. The linking by the midlatitude teleconnection is likely helpful to a better understanding of the tropical and subtropical monsoons, and needs to be further clarified in the future studies.

We also examined the teleconnections in half-month mean, and in June, August and JJA, and found similar patterns with slightly unclear structures in comparison to the July pattern. Moreover, we did not find any clear relationship between this Rossby wave and ENSO events.

7. Acknowledgements

Research work was supported by the Chinese Academy of Sciences under contract KZCX2-203. Part of work was done during R.-Y.L.'s visit to the Forecast Research Laboratory of Meteorological Research Institute of Korea Meteorological Administration (FRL/METRI/KMA). His visit was supported by the Brain Pool Program (grant no. 991-5-8) founded by the Korea Science and Engineering Foundation, and by the Natural Hazard Prevention Research Project, one of the Critical Technology-21 Programs, funded by the Ministry of Science and Technology of Korea. R.-Y.L. gratefully appreciates the faculty in FRL/METRI for their help during his stay. The authors are grateful to anonymous reviewers for useful comments that led to most of the research work in Section 4.

Table 1. *Comparison of the teleconnection pattern in meridional wind identified in the present study with those in other elements, such as geopotential height, streamfunction and vorticity, identified in the previous studies (Wallace and Gutzler, 1981; Blackmon et al., 1984a, b; Kiladis and Weickmann, 1992; Hsu and Lin, 1992; Hoskins and Ambrizzi, 1993; Ambrizzi et al., 1995). The teleconnection patterns in the previous studies are separated into intermediate- and low-frequency fluctuations*

	Present	Intermediate	Low
Period (days)	>30	10–30	>30
Zonal wavenumber	7	7 (Ambrizzi et al., 1995)	1–4 (in winter)
Mode of spatial organization	Geographically fixed wave trains along waveguides of jet streams	Mobile wave trains along waveguides of jet streams	Geographically fixed north–south dipole patterns straddling either the jet exit or the equator
Mode of time variation	Trapped over East Asia	Dispersion through stationary wave trains	Not well-defined

REFERENCES

Ambrizzi, T., Hoskins, B. J. and Hsu, H.-H. 1995. Rossby wave propagation and teleconnection patterns in the austral winter. *J. Atmos. Sci.* **52**, 3661–3672.

Annamalai, H., Slingo, J. M., Sperber, K. R. and Hodges, K. 1999. The mean evolution and variability of the Asian summer monsoon: Comparison of ECMWF and NCEP-NCAR reanalyses. *Mon. Wea. Rev.* **127**, 1157–1186.

Blackmon, M. L., Lee, Y.-H. and Wallace, J. M. 1984a. Horizontal structure of 500 mb height fluctuations with long, intermediate and short timescales. *J. Atmos. Sci.* **41**, 961–980.

Blackmon, M. L., Lee, Y.-H., Wallace, J. M. and Hsu, H.-H. 1984b. Time variation of 500 mb height fluctuations with long, intermediate and short time scales as deduced from lag-correlation statistics. *J. Atmos. Sci.* **41**, 981–991.

Guo, Q. Y. and Wang, J. 1988. A comparative study on summer monsoon in China and Indian. *J. Tropical Meteorol.* **4**, 53–60 (in Chinese with English abstract).

Hoskins, B. J. and Ambrizzi, T. 1993. Rossby wave propagation on a realistic longitudinally varying flow. *J. Atmos. Sci.* **50**, 1661–1671.

Hsu, H.-H. and Lin, S.-H. 1992. Global teleconnections in the 250-mb streamfunction field during the Northern Hemisphere winter. *Mon. Wea. Rev.* **120**, 1169–1190.

Joseph, P. V. and Srinivasan, J. 1999. Rossby waves in May and the Indian summer monsoon rainfall. *Tellus* **51A**, 854–864.

Kalnay, E., Kanamitsu, M., Kristler, R., Collins, W., Deaven, D., Gandin, L., Iredell, M., Saha, S., White, G., Woollen, J., Zhu, Y., Chelliah, M., Ebisuzaki, W., Higgins, W., Janowiak, J., Mo, K. C., Ropelewski, C., Wang, J., Leetmaa, A., Reynolds, R., Jenne, R. and Jesoph, D. 1996. The NCEP/NCAR 40-year reanalysis project. *Bull. Am. Meteorol. Soc.* **77**, 437–471.

Kiladis, G. N. and Weickmann, K. M. 1992. Circulation anomalies associated with tropical convection during Northern winter. *Mon. Wea. Rev.* **120**, 1900–1923.

Kripalani, R. H. and Singh, S. V. 1993. Large scale aspects of Indian–China summer monsoon rainfall. *Adv. Atmos. Sci.* **10**, 71–84.

Parthasarathy, B., Rupakumar, K. and Deshpande, V. R. 1991. Indian summer monsoon rainfall and 200 mb meridional wind index application for long range prediction. *Int. J. Climatol.* **11**, 165–176.

Tao, S. Y. and Chen, L. X. 1987. A review of recent research on the East Asian summer monsoon in China. In: *Review in monsoon meteorology* (eds. C.-P. Chang and T. N. Krishnamurti). Oxford University Press, Oxford, 60–92.

Wallace, J. M. and Gutzler, D. S. 1981. Teleconnections in the geopotential height field during the Northern Hemisphere winter. *Mon. Wea. Rev.* **109**, 785–812.

Xie, P. and Arkin, P. A. 1997. Global precipitation: A 17-year monthly analysis based on gauge observations, satellite-estimates, and numerical model outputs. *Bull. Am. Meteorol. Soc.* **78**, 2539–2558.